CONCENTRIC TUBE-FOULING RIG FOR INVESTIGATION OF FOULING DEPOSIT FORMATION FROM PASTEURISER OF VISCOUS FOOD LIQUID

N. I. KHALID, K. W. CHAN, N. AB AZIZ*, F. S. TAIP, M. S. ANUAR

Department of Process and Food Engineering, Faculty of Engineering,
Universiti Putra Malaysia, 43400 Serdang, Selangor Darul Ehsan, Malaysia
*Corresponding Author: shekeen@eng.upm.edu.my

Abstract

This paper reports the work on developing concentric tube-fouling rig, a new fouling deposit monitoring device. This device can detect and quantify the level of fouling deposit formation. It can also functioning as sampler for fouling deposit study, which can be attached at any food processing equipment. The design is initiated with conceptual design. The rig is designed with inner diameter of 7 cm and with tube length of 37 cm. A spiral insert with 34.5 cm length and with 5.4 cm diameter is fitted inside the tube to ensure the fluid flows around the tube. In this work, the rig is attached to the lab-scale concentric tube-pasteurizer to test its effectiveness and to collect a fouling sample after pasteurization of pink guava puree. Temperature changes are recorded during the pasteurization and the data is used to plot the heat transfer profile. Thickness of the fouling deposit is also measured. The trends for thickness, heat resistance profile and heat transfer profile for concentric tube-fouling rig matched the trends obtained from lab-scale concentric tube-pasteurizer very well. The findings from this work have shown a good potential of this rig however there is a limitation with spiral insert, which is discussed in this paper.

Keywords: Fouling deposit, Fouling rig, Viscous fluids, Pasteurization, Pink guava puree.

1. Introduction

Fouling deposit or also known in some industries as scale is the accumulation of unwanted deposits on the surfaces of processing equipment. Fouling deposit is an unwanted by-product of most process industries, such as food, petroleum and water treatment industries. This is particularly a severe problem especially in food

Nomenclatures

A	Cross sectional area of fouling deposit, m^2
c_p	Specific heat of fouling deposit, $Jkg^{-1}{}^{\circ}C^{-1}$
d	Diameter of the inner concentric tube-fouling rig, m
k_f	Thermal conductivity of fouling deposit, $Wm^{-1}{}^{\circ}C^{-1}$
L	Length of the concentric tube-fouling rig, m
m	Mass of fouling deposit, kg
$\dot{m}$	Mass flow rate of product, kgs^{-1}
Q	Heat transfer , Js^{-1}
R_f	Fouling resistance , $W^{-1}m^2{}^{\circ}C$
R_{fa}	Average fouling resistance , $W^{-1}m^2{}^{\circ}C$
R_{ft}	Theoretical fouling resistance , $W^{-1}m^2{}^{\circ}C$
U	Overall heat transfer coefficient, $Wm^{-2}{}^{\circ}C^{-1}$
U_o	Initial overall heat transfer coefficient, $Wm^{-2}{}^{\circ}C^{-1}$
V	Volume of fouling deposit, m^3
X_f	Thickness of fouling deposit, m
X_{fa}	Average thickness of fouling deposit, m
X_{ft}	Theoretical thickness of fouling deposit, m

Greek Symbols

ΔT	Temperature changes of product, $^{\circ}C$
ΔT_1	Temperature oil out – temperature product in ,$^{\circ}C$
ΔT_2	Temperature oil in – temperature product out, $^{\circ}C$
ρ	Density of fouling deposit, kgm^{-3}

and milk industries where frequent cleaning is needed [1]. The formation of food fouling deposit is rapid in heat exchanger. This deposit affects the heat transfer and causing the resistance to the process fluid to flow. Thus fouling deposit can give bad effect to the process environment and the cost of the production. There are many factors that can promote fouling deposit formation, such as the process parameters, raw material properties and the fluid processing mechanics [2, 3].

Currently the best method in food industries to remove fouling deposit is by performing cleaning-in-place (CIP). However a long and frequent CIP is not economic. The information on fouling deposit condition is often used as the basis for finding the suitable CIP procedure. Hence, an appropriate monitoring device and method are important to detect and quantify the level of fouling deposit formation. There are several constraints need to consider in designing the monitoring device such as the configuration, the material, the operation parameters of the processing equipment and the not uniformed fouling deposit distribution.

Previous works have designed rigs and methods for monitoring the fouling deposit. Mainly the designs provide in-direct measurements, by using heat flux sensor [4, 5]. Truong et al. [4] stated that the sensor can be attached at different locations in plant without disturbing the plant operations. However this sensor cannot be mounted at heating area, where the formation of fouling deposit is significant. Ultrasonic waves are also used for monitoring fouling [6]. To detect fouling, Withers [7] explain a good summary by using ultrasonic bulk wave techniques. By using ultrasonic inspection, McClements [8] also provides

summary on measuring thickness to particle sizing. However, thin, not homogeneous and rough deposits are difficult to detect and may produce high signal noise. Besides, the installation of the devices for ultrasonic inspection in heating area is also not possible. Different method used based on differential turbidity, light scattering, heat transfer and pressure drop, radiations signals (spectroscopy, fluorometry, photo acoustic spectroscopy, etc.) and electric signals for online biofilm monitoring techniques [9]. Each methods has its own detection limit and used for different situations. For example, nuclear magnetic resonance and photo acoustic spectroscopy can be considered if both physical structure and chemical properties are important.

Thus, the main objective of this work is to fabricate a monitoring device for fouling deposit, namely concentric tube-fouling rig, which provides in-direct measurement at heating area. The concentric tube-fouling rig is attached to the lab-scale concentric tube-pasteurizer to test its effectiveness and to collect a fouling sample after pasteurization of pink guava puree.

2. The Proposed Design

The basic idea of the design is to design a rig that allows an in-direct measurement at heating area and can be dismantled easily to monitor the fouling deposit. It is also functioning as sampler for fouling deposit study, which can be attached at any food processing equipment. The technical drawing of the concentric tube-fouling rig is shown in Fig. 1. This design has larger size of cross sectional area compared to common tubular heat exchanger in the industry and to the lab-scale concentric tube-pasteurizer [10] that is used in the laboratory for current studies. The inner diameter of lab-scale concentric tube-pasteurizer is 2.25 cm and the length is 100 cm. While, the concentric tube-fouling rig is designed with inner diameter of 7 cm and length of 37 cm. Thus, a good picture of the fouling deposit accumulated on the stainless steel surface of the rig can be obtained.

A spiral is inserted in the tube to ensure that the pink guava puree flows around the tube. Figure 2 shows the technical drawing of the spiral inserted into the concentric tube-fouling rig. Figure 3 shows the concentric tube-fouling rig and its parts. Pink guava purees flow in concentric tube-fouling rig through reducer 1 and enters concentric tube 1. Then, it flows through the concentric tube 2. Lastly, it flows out through reducer 2. Figure 4 shows the difference between the cross sectional area of the concentric tube-fouling rig and the lab-scale concentric tube-pasteurizer.
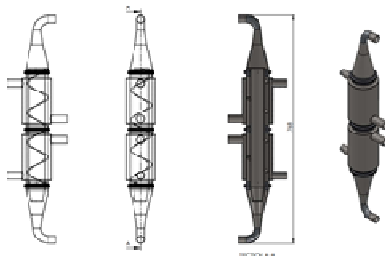
Fig. 1. Technical Drawing of the Concentric Tube-Fouling Rig.
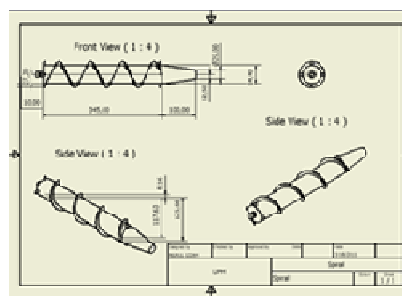
Fig. 2. Technical Drawing of the Spiral.
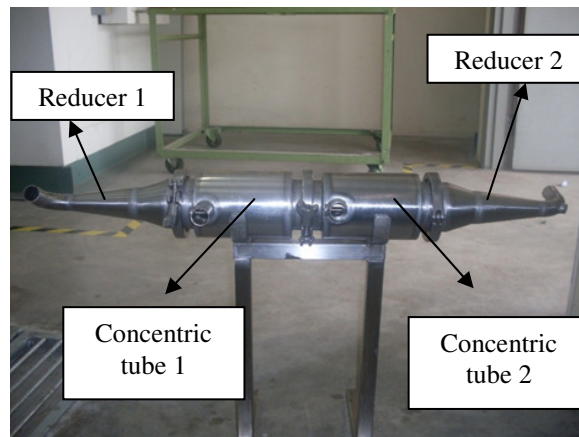
Fig. 3. Concentric Tube-Fouling Rig.

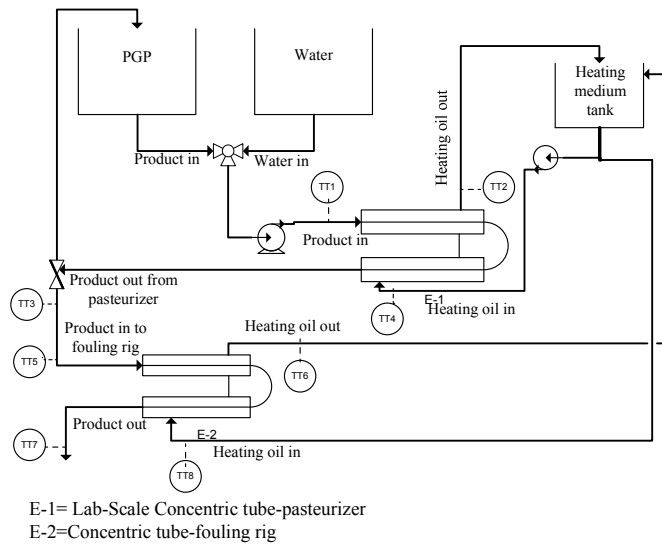**(a) Concentric Tube-Fouling Rig.**   **(b) Lab-scale Concentric Tube-Pasteurizer.**

Fig. 4. Cross-sectional Area Difference.

3. Material and Methodology

Pink guava puree is supplied by Sime Darby Beverages Sdn. Bhd. (Sitiawan, Malaysia) and it is used as a fluid model in this study.

Prior to pasteurization, the concentric tube-fouling rig is attached to the final tube of the concentric tube-lab-scale pasteurizer, which has found to produce maximum fouling build-up. Pink guava puree is pasteurized between 90 to 95°C with volumetric flow rate of 0.3 L/min and holding time at 90 seconds. The lab-scale concentric tube–pasteurizer is operated for 6 hours for ensuring sufficient fouling data can be obtained.

Every part of concentric tube-fouling rig is dismantled after every hour of pasteurization for observation. Temperature changes are recorded and the results are used to plot the heat transfer and heat resistance profiles. Thickness of the fouling deposit is also measured. Figure 5 shows the Process Flow Diagram (PFD) of the experimental process.

E-1= Lab-Scale Concentric tube-pasteurizer
E-2=Concentric tube-fouling rig

Fig. 5. Process Flow Diagram of the Concentric Tube-Fouling Rig that is Attached to the Lab-Scale Concentric Tube-Pasteurizer.

The average thickness of the fouling deposit X_{fa} is calculated by using Eq. (1). The cross sectional area can be calculated by using Eq. (2). The weight of the fouling deposit is weighed for every 1 hour. The density of the fouling deposit is determined during the experiment and is calculated by using Eq. (4). The thickness of fouling deposit vs. time is plotted in Fig. 9.

$$X_{fa} = \frac{m}{A} \times \frac{1}{\rho} \tag{1}$$

Cross sectional area of the fouling deposit flow is determined by calculating the inner surface of the fouling rig-concentric tube.

$$A = \pi dL \tag{2}$$

By using the value of X_{fa}, the average fouling resistance R_{fa} is determined by using Eq. (3). A graph of fouling resistance vs. time is plotted in Fig. 10.

$$R_{fa} = \frac{X_{fa}}{k_f} \tag{3}$$

The density of the fouling deposit is determined to calculate the average thickness of the fouling deposit. The density of the fouling deposit is determined by using beaker. 20 ml of fouling deposit is taken and the weight of the fouling deposit is weighed. The density is calculated by using Eq. (4).

$$\rho = \frac{m}{V} \tag{4}$$

The theoretical thickness and fouling resistance of the fouling deposit is determined from the heat transfer data that is taken at every 3 minutes. The overall heat transfer coefficient is also calculated from the data. The theoretical thickness of the fouling deposit X_{ft} can be determined by using Eq. (5). Graph of thickness of fouling deposit vs. time is plotted in Fig. 9.

$$X_{ft} = R_{ft} \times k_f \tag{5}$$

The fouling resistance or fouling factor R_f can be determined by using Eq. (6). A graph of fouling resistance vs. time is plotted in Fig. 10.

$$R_{ft} = \frac{1}{U} - \frac{1}{U_0} \tag{6}$$

The overall heat transfer coefficient can be determined from Eq. (8). The value of heat transfer is determined from Eq. (9). Graph of overall heat transfer coefficient vs. time is plotted in Fig. 11.

$$\Delta T_{lm} = \frac{\Delta T_1 - \Delta T_2}{\ln \frac{\Delta T_1}{\Delta T_2}} \tag{7}$$

$$U = \frac{Q}{A \ x \ \Delta T_{lm}} \tag{8}$$

The heat transfer between the fluids is determined by using Eq. (9).

$$Q = \dot{m} c_p \Delta T \tag{9}$$

4. Results and Discussion

4.1. Monitoring the fouling deposit

The photos of the fouling deposit at concentric tube 1, concentric tube 2 and reducer 2 for every hour are taken and are shown in Figs. 6 -8 respectively. There is no fouling deposit accumulated on the surface of reducer 1.


| (a) 1st Hour | (b) 2nd Hour | (c) 3rd Hour |

| (d) 4th Hour | (e) 5th Hour | (f) 6th Hour |
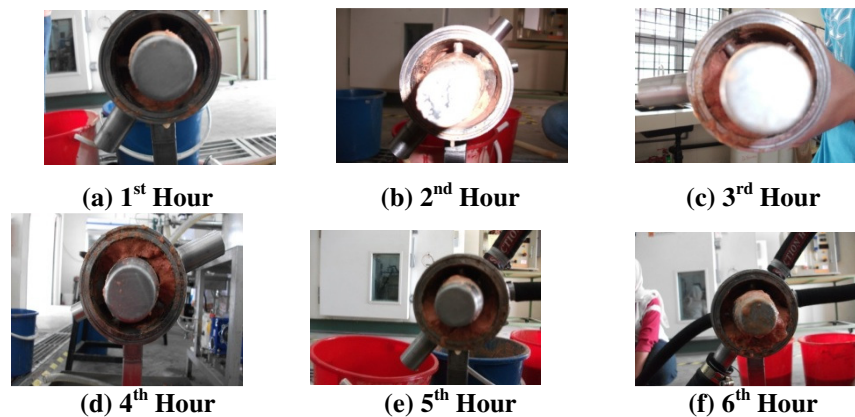
Fig. 6. Photos of Fouling Deposit Accumulated on the Surface of Concentric Tube 1 at Different Hours.

(a) 1st Hour   **(b) 2nd Hour**   **(c) 3rd Hour**

(d) 4th Hour   **(e) 5th Hour**   **(f) 6th Hour**
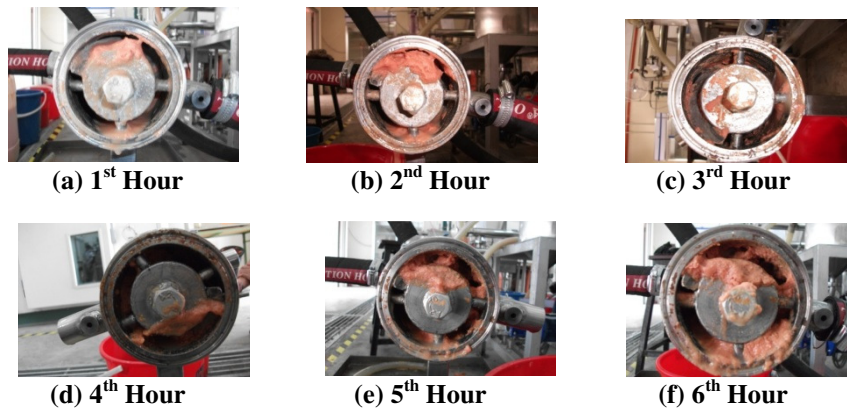
**Fig. 7. Photos of Fouling Deposit Accumulated
on the Surface of Concentric Tube 2 at Different Hours.**

From the tables, the fouling deposit started to accumulate at the first hour on the surface of concentric tube 1, concentric tube 2 and reducer 2. Then, for the next hours, the fouling deposit accumulates on the initial layer of the fouling deposit and it continued until the sixth hour. Concentric tube 1, concentric tube 2 and reducer 2 show the same result. As time increase, the fouling deposit accumulated on the surface of the concentric tube 1, concentric tube 2 and reducer 2 also increase.

(a) 1st Hour   **(b) 2nd Hour**   **(c) 3rd Hour**

(d) 4th Hour   **(e) 5th Hour**   **(f) 6th Hour**
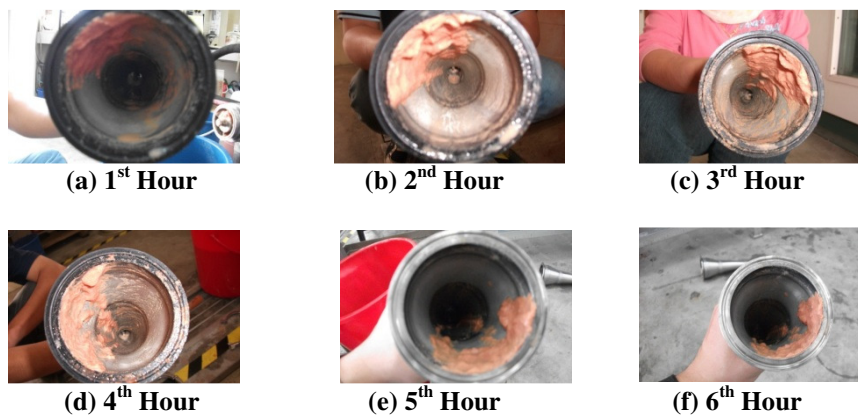
**Fig. 8. Photos of Fouling Deposit Accumulated
on the Surface of Reducer 2 at Different Hours.**

In addition, other than observing the changes of the thickness of the fouling deposit, the fouling deposit can be collected to determine the density of the fouling deposit in this work. It also can be collected to study other properties such thermal conductivity and specific heat capacity.

However, the fouling deposit accumulated on the center of the concentric tube-fouling rig cannot be observed due the spiral provides a barrier to monitor the fouling deposit. This is due to the difficulty to remove the spiral without disturbing the fouling deposit structure. Furthermore, as the temperature increase during the pasteurization process, the spiral expands in the tube and makes the spiral hard to be pulled out.

From the observation, the fouling rig is capable to accumulate the fouling deposit. There are advantages and disadvantages for this design. The main advantages are the similar configuration to the lab-scale concentric tube-pasteurizer and the material of construction which comply the food regulation. Thus, the measurement is more accurate to represent the process environment in the real tubular heat exchanger. The fouling deposit can be monitored and the sample of the fouling deposit can be collected to be used in determining several significant properties. Furthermore, the installation of this fouling rig to existing unit operation does not required major modification and the requirement for skill and training in employing this rig is not extensive than with some other methods. But the spiral insert becomes an obstacle to observe the fouling deposit accumulated on the surface of the tube.

4.2. Monitoring the thickness profile

A graph of theoretical thickness and average thickness of fouling deposit for concentric tube-fouling rig versus time is shown in Fig. 9. The profile of theoretical thickness of fouling deposit vs. time for lab-scale concentric tube-pasteurizer is also shown in Fig. 9. A graph of fouling resistance versus time is shown in Fig. 10. The theoretical thickness is calculated from heat transfer data. The average thickness and theoretical thickness for both lab-scale concentric tube-pasteurizer and concentric tube-fouling rig have shown similar trend. After 300 minutes the theoretical thickness for concentric tube-fouling rig is significantly higher than the average thickness for concentric tube-fouling rig and the theoretical thickness of the lab-scale concentric tube-pasteurizer. The method to obtain theoretical thickness is depending on the sensitivity of the thermocouple and the location of it. The accumulation of the fouling deposit on the spiral insert can also influence this result.

The average thickness of the fouling deposit is determined from the weight of the fouling deposit. The weight is measured after every hour of the experiment. Fig. 9 shows that as time increase, the average thickness of the fouling deposit is increased. Thus, it agrees with Bott [2] finding which stated that, as time increase, the fouling deposit accumulated on the surface of heat exchanger is also increased.

The results shows that the theoretical thickness obtained from lab-scale concentric tube-pasteurizer is lower compared to average and theoretical thickness of fouling deposit from the concentric tube-fouling rig. The spiral insert may influence the data for average thickness. As the weight obtain is included the weight of the fouling deposit in the concentric tube-fouling rig and the weight of the fouling deposit accumulated on the surface of the spiral.
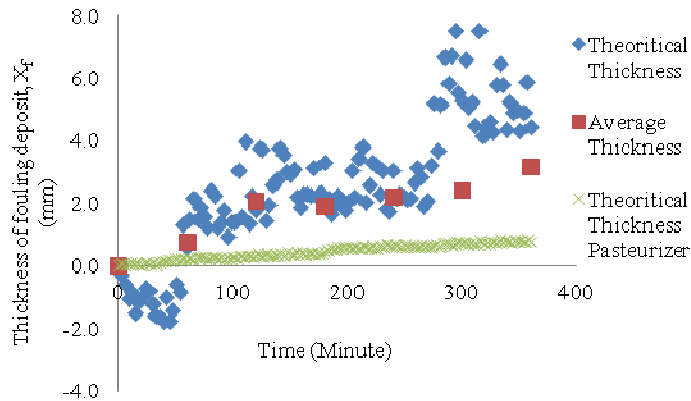
The trend of theoretical thickness for both lab-scale concentric tube-pasteurizer and concentric tube-fouling rig shows similar trend. This finding supports the compatibility of this rig for fouling study.

4.3. Monitoring the heat transfer profile

As the fouling deposit thickness increasing, the fouling resistance is also increasing. Figure 10 shows that as the time increases, the fouling resistance is increasing. The fouling deposit provides the heat transfer resistance and reduces

the effectiveness of the heat transfer due the pressure drop that increases inside the heat exchanger [2].

Fig. 9. The Changes of Fouling Deposit Thicknesses in Concentric Tube-Fouling Rig and Lab-Scale Concentric Tube-Pasteurizer.
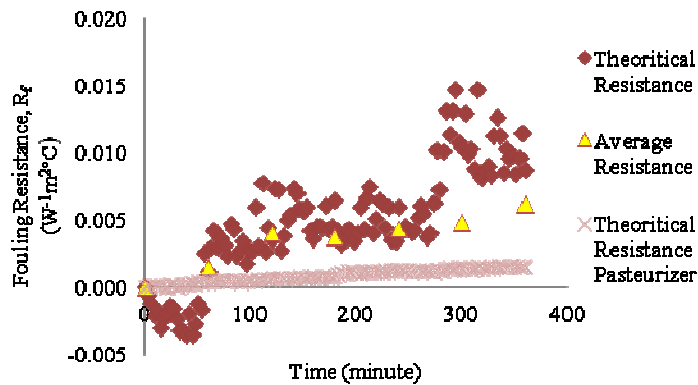

Fig. 10. Theoretical and Experimental Fouling Resistance Profiles.

Theoretical fouling resistance for both lab-scale concentric tube-pasteurizer and concentric tube-fouling rig shows similar trend. Thus, it proves that this rig can be used for fouling study. However, the theoretical and average thickness for concentric tube-fouling rig is significantly higher than the theoretical thickness of the lab-scale concentric tube-pasteurizer. The calculation in determining fouling resistance depends on the value of the fouling thickness. Since the weight of fouling deposit is affected with the spiral insert, it directly affects the value of the fouling resistance.

This result reflects the effect of increase in fouling deposit thickness towards the heat transfer. As the fouling deposit thickness increased, the fouling resistance is increasing, result in decrease of heat transfer coefficient. Besides, the cross sectional area of the heat exchanger is reduced and causes an increase in pressure drops. Significant pressure drop increment can increase the power needed to pump the

processing fluid and moreover it can damage the processing equipment [2]. Figure 11 shows that the intensity profile of heat transfer coefficient for lab-scale concentric tube-pasteurizer is higher compared to concentric tube-fouling rig. The fouling resistance for lab-scale concentric tube-pasteurizer is lower, thus it heat transfer coefficient is higher. The decrease in the thermal performance of the heat exchanger will leads to incomplete product heating and product loss. Thus, cleaning in place for heat exchanger equipment is used to solve these problems [11].
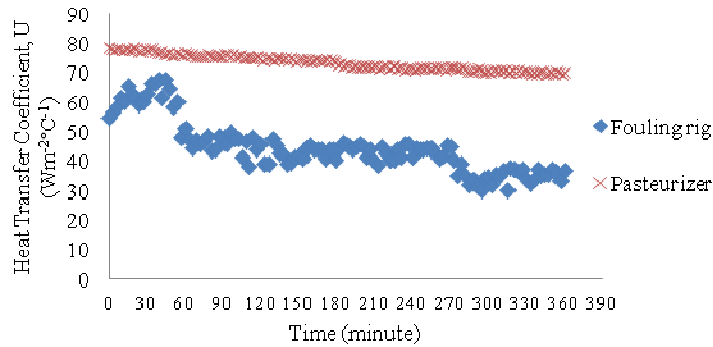
Fig. 11. Heat Transfer Coefficient Profiles for Concentric Tube-Fouling Rig and Lab-Scale Concentric Tube-Pasteurizer.

5. Conclusions

Concentric tube-fouling rig is designed to monitor the viscous fluid fouling deposit formation on the surface of the tubular heat exchanger. It is also functioning as sampler for fouling deposit study and it can be attached at any tubular type heat exchanger. This paper has proven that this concentric tube -fouling rig has potential to be used as fouling monitor at any complex processing line where frequent dismantling is laboured and impossible. Besides, the requirement for skill and training in employing this rig is not extensive than with some other methods.

Recommendation for future work is to improve the design of the spiral insert for ensuring the measurement for the fouling thickness is feasible.

Aknolwedgment

References

1. Visser, J.; and Jeurnink, T.J.M. (1997). Fouling of heat exchangers in the dairy industry. *Experimental Thermal and Fluid Science*, 14(4), 407-424.
2. Bott, T.R. (2009). *Fouling of heat exchanger*. University of Birmingham, Birmingham, UK.

3. Simmons, M.J.H.; Jayaraman P.; and Fryer, P.J. (2007). The effect of temperature and shear rate upon the aggregation of whey protein and its implications for milk fouling. *Journal of Food Engineering*, 79(2), 517-528.

4. Truong, T.; Anema, S.; Kirkpatrick, K.; and Chen, H. (2002). The use of a heat flux sensor for in-line monitoring of fouling of non-heated surface. *Food and Bioproducts Processing*, 80(4), 260-269.

5. Davies, T.J.; Henstridge, S.C.; Gillham, C.R.; and Wilson, D.I. (1997). Investigation of whey protein deposit properties using heat flux sensors. *Food and Bioproducts Processing*, 75(2), 106-110.

6. Hay, T.R.; and Rose, J.L. (2003). Fouling detection in the food industry using ultrasonic guided waves. *Food Control*, 14(7), 481-488.

7. Withers, P.M. (1996). Ultrasonic, acoustic and optical techniques for the non-invasive detection of fouling in food processing equipment. *Trends in Food Science and Technology*, 7(9), 293-298.

8. McClements, D.J. (1995). Advances in the application of ultrasound in food analysis and processing. *Trends in Food Science and Technology*, 6(9), 293-299.

9. Janknecht, P.; and Melo, L.F. (2003). Online biofilm monitoring. *Reviews in Environmental Science and Bio/Technology*, 2(2-4), 269-283.

10. Lee, C.M. (2009). *A bench-scale tubular heat exchanger design for experimental study*. Bachelor Thesis. Universiti Putra Malaysia, Malaysia.

11. Tamime, A.Y. (2008). *Cleaning in place: Dairy, food and beverages operation*. (3rd Ed.), Blackwell publishing, Oxford, UK.